Corrections to the free-nucleon values of the single-particle matrix elements of the $M1$ and Gamow-Teller operators, from a comparison of shell-model predictions with sd-shell data

B. A. Brown and B. H. Wildenthal

Cyclotron Laboratory, Michigan State University, East Lansing, Michigan 48824

The magnetic dipole moments of states in mirror pairs of the sd-shell nuclei and the strengths of the Gamow-Teller beta decays which connect them are compared with predictions based on mixed-configuration shell-model wave functions. From this analysis we extract the average effective values of the single-particle matrix elements of the l, s, and $[Y^{(2)} \otimes s]^{(1)}$ components of the $M1$ and Gamow-Teller operators acting on nucleons in the $0d_{5/2}$, $1s_{1/2}$, and $0d_{3/2}$ orbits. These results are compared with the recent calculations by Towner and Khanna of the corrections to the free-nucleon values of these matrix elements which arise from the effects of isobar currents, mesonic-exchange currents, and mixing with configurations outside the sd shell.

RADIOACTIVITY $A = 17-39$ nuclei, magnetic dipole moments and Gamow-Teller beta-decay strengths; shell-model wave functions, complete $0\hbar\omega$ $0d_{5/2}$-$1s_{1/2}$-$0d_{3/2}$ basis space, empirical Hamiltonian; extraction of empirical normalizations of the l, s, and $[Y^{(2)} \otimes s]^{(1)}$ single-particle operators.

I. INTRODUCTION

Our goal in this study is to extract empirical values of the single-particle matrix elements of the Gamow-Teller (GT) and magnetic dipole $(M1)$ operators from a set of interrelated nuclear data. We concentrate on sd-shell nuclei which are removed by two or more nucleons from the $A = 16$ and 40 major shell closures and on states for which the isovector and/or isoscalar magnetic dipole moments are available. We are particularly concerned with those examples for which both isovector $M1$ and GT data can be obtained for the same (in the sense of isospin symmetry) nuclear state.

We interpret our chosen data in the context of shell-model wave functions whose dimensions span all $0d_{5/2}$-$1s_{1/2}$-$0d_{3/2}$ configurations. From these wave functions we calculate for each nuclear state ATJ in our data set the five isovector and/or five isoscalar matrix elements of the $\Delta J^\pi = 1^+$ one-body operators of the model space. The appropriate sums of the products of these N-body matrix elements with the single-particle matrix elements of the $M1$ and GT operators yield total matrix elements which should correspond to experimental values. We extract the empirically best values of the single-particle matrix elements from least-squares fits of the linear combinations of the N-body shell-model matrix elements to the experimental values.

This analysis should produce information about these single-particle matrix elements which is analogous to what can be obtained from the simpler analyses which are possible for the data of the "single-particle" and "single-hole" (in the context of the usual shell-model assumptions) states of $A = 17$ and 39, respectively. In the conventional assumption of shell closures at $A = 16$ and 40 (which we

also utilize in the present work) each relevant experimental value from $A = 17$ and 39 can be related to only one single-particle matrix element of the appropriate operator, rather than five.

At the least, the results of our present analysis of data from $A = 18$ to 38 will provide independent alternative values against which to compare the values obtained from $A = 17$ and 39 and, as well, provide new information about terms which cannot be measured in these systems. At best, this analysis of multiparticle data may provide results which are less subject to nuclear-model uncertainties than are those obtained from the single-particle systems. Idiosyncrasies in either the data or the theory will be averaged out to some degree by virtue of the larger sampling of states available from the "interior" of the shell. Moreover, the descriptions of these multiparticle states appear to be relatively free from the uncertainties associated with the "intruder state" contaminations which arise from many-particle, many-hole excitations across the nominal shell boundaries.

The empirical values for the single-particle matrix elements of the $M1$ and GT operators which we deduce from the present analysis are to be viewed in comparison with the values which are obtained by assuming that the "nucleons" of the model description have the observed magnetic moments of the free neutron and proton and Gamow-Teller properties consistent with the half-life of the free neutron. Deviations of our empirically-based values from these "free-nucleon" numbers should reflect inadequacies in the theoretical model which we utilize in the analysis of the data. We distinguish three levels of inadequacy in the shell-model predictions. The lowest corresponds to the failure of our specific version of sd-shell model wave functions to match the "best-in-

principle" results possible with the same general model assumptions. The next level of inadequacy corresponds to the basic limitations arising from the restriction of the model space to a single major oscillator shell. On the most fundamental level, the inadequacies of the model we use include its assumptions of the impulse approximation and the omission of coordinates other than neutron and proton.

We necessarily assume for our present purposes that the shell-model wave functions we employ are close approximations to the best results obtainable within our model constraints. The differences between the empirical values for the single-particle matrix elements which we deduce from least-squares fits to data and the free-nucleon values then must be attributed to the necessity of making higher-order corrections to the conventional shell-model representation in order to compensate for the second and third levels of inadequacies in the conventional model. These estimates of higher-order corrections are of current interest relative to several theoretical programs aimed at calculating the effects which the restriction of the basis space to a single major oscillator shell and the presence in nature of mesonic-exchange current and isobar-excitation contributions have upon the relationship between "simple" model predictions and experimental values. We will compare our results in detail with the recent calculations of Towner and Khanna.[1] The results and conclusions of the Towner-Khanna calculations are in good agreement with those previously carried out by Arima, Hyuga, Ichimura, and Shimizu,[2-4] and we refer the reader to these references for further details.

The essence of our approach is the assumption that "good" configuration-mixing shell-model calculations for $M1$ and GT phenomena, when combined with the free-nucleon parametrizations of these operators, should account for much of the detail observed in the variation from state to state of the relative sizes of the magnetic moments and Gamow-Teller strengths and, more qualitatively, for their average absolute magnitudes. This assumption has been validated in a series of extensive studies.[5,6] We then follow this initial assumption with the assumption that the residual discrepancies between these shell model predictions and the experimental values are properly removed by the introduction of essentially state-independent perturbative corrections to the specifications of the $M1$ and GT operators or, equivalently, to their single-particle matrix elements.

It should be noted that these perturbative corrections also can give rise to effective many-body $M1$ and GT operators within the model space. We ignore such effects to the extent that they cannot be encompassed within a smooth mass dependence of the parameters. The sizes and importance of these explicit many-body effects which are inferred from our analysis and from calculations will be discussed in Sec. VI.

The antecedents of the present study are the pioneering papers of Wilkinson[7,8] and their subsequent elaborations by Brown, Chung, and Wildenthal.[9,6] Several different sets of data on GT beta decay and magnetic dipole moments were used in these previous investigations, in conjunction with progressively evolving shell-model wave

functions for sd-shell nuclei. We utilize here the latest generation of wave functions in this theoretical evolution[10] together with a set of data which we have shown to optimize experimental precision, model reliability, and the possibility of internally cross validating the results of the analyses.

In Sec. II we define generalized expressions for the $M1$ and GT operators in which parameters corresponding to higher-order corrections to the free-nucleon values occur explicitly. In Sec. III we present the results of the shell-model calculations for the $M1$ and GT observables and the values obtained for the corrections to the free-nucleon values which we obtain from the least-squares fits to the experimental observables. In Sec. IV we discuss in detail the relationships between the experimental and calculated observables. In Sec. V we compare our empirically obtained higher-order corrections with recent calculations of these quantities. Conclusions and a discussion of future prospects are given in Sec. VI.

II. DEFINITION OF THE OPERATORS AND CORRECTION PARAMETERS

The data we consider in the present study are the magnetic dipole moments (μ) of $T=0$ states and of pairs of $T_Z = \pm T$ states of $A=18-38$ nuclei and the strengths of the GT beta decays which connect the $T_Z = +\frac{1}{2}$ members of mirror pairs to their $T_Z = -\frac{1}{2}$ reflections. We separately consider the analogous data from $A=17$ and 39. We analyze these experimental data by constructing sets of least-squares-fit equations in which the shell-model expressions for $M1$ and GT matrix elements are matched to the corresponding measured values. In the present cases, for which the data can be projected into purely isoscalar and purely isovector combinations, these equations relate an observable ($\mathscr{E}$) to a linear combination of the products of reduced single-particle matrix elements ($S_{jj'}^{Op}$) for the relevant operator (Op) and the one-body transition densities ($D_{jj'}$) calculated from the N-particle shell-model wave function

$$\mathscr{E} = C(\mathscr{E}, i, f) \sum_{jj'} S_{jj'}^{Op} D_{jj'}(\Delta T, \Delta J, i, f) . \tag{1}$$

In Eq. (1) Op indicates either the isoscalar ($\Delta T = 0$) $M1$ operator (ISM1), the isovector ($\Delta T = 1$) $M1$ operator (IVM1), or the isovector Gamow-Teller (GT) operator, all of which have $\Delta J = 1$. These operators will be specified in detail below. The complete sets of quantum numbers $ATJ\nu$ which label the initial and final shell-model states are indicated by the letters i and f ($i = f$ in the cases considered here), and j and j' identify the orbits $\rho(nlj)$ of the shell-model space. $C(\mathscr{E}, i, f)$ is a fixed numerical coefficient which connects the theoretical value of a particular observable to the reduced matrix element of the associated operator.

We express the $M1$ and GT observables in terms of the isoscalar and isovector magnetic moments μ(ISM1/IVM1) and the GT beta-decay matrix elements M(GT). These are defined by the equations

$$\mu(\text{ISM1}/\text{IVM1}) = [\mu(T_Z = +T) \pm \mu(T_Z = -T)]/2 \ , \tag{2}$$

and

$$M(\text{GT}) = [(2J_i + 1)B(\text{GT})]^{1/2} \ . \tag{3}$$

The $\mu(T_Z)$ are the magnetic dipole moments in units of nuclear magnetons, where our convention is that $T_Z = +\frac{1}{2}$ for the proton. The $B(\text{GT})$ are related to the partial half-lives for beta decay, $t_{1/2}$, by

$$t_{1/2} = \frac{6170 \pm 4}{f_V B(\text{F}) + f_A B(\text{GT})} \tag{4}$$

The $B(\text{F})$ are the Fermi beta-decay nuclear matrix elements and the terms f_V and f_A are the vector (V) and axial-vector (A) beta-decay phase space factors; details of the calculations of these quantities are given in Refs. 11, 7, and 12.

For the $M1$ moments, the coefficient in Eq. (1) is given by the 3-j symbols

$$C[\mu(\text{ISM1}/\text{IVM1})] = \begin{bmatrix} J & 1 & J \\ -J & 0 & J \end{bmatrix} \begin{bmatrix} T & \Delta T & T \\ -T & 0 & T \end{bmatrix} . \tag{5}$$

For the $T_Z = \frac{1}{2}$ to $T_Z = -\frac{1}{2}$ GT decay, the isospin vector-coupling coefficient reduces to

$$C(\text{GT}) = (\tfrac{2}{3})^{1/2} \ . \tag{6}$$

The $D_{jj'}(\Delta T, \Delta J, i, f)$ are obtained from shell-model wave functions according to

$$D_{jj'}(\Delta T, \Delta J, i, f) = \frac{\langle f |||[a^\dagger(j) \times \tilde{a}(j')]^{\Delta J, \Delta T}|||i \rangle}{[(2\Delta J + 1)(2\Delta T + 1)]^{1/2}} \ . \tag{7}$$

The calculations which produced these wave functions utilize the full space of $0d_{5/2}\text{-}1s_{1/2}\text{-}0d_{3/2}$ configurations and the A-dependent empirical effective Hamiltonian of Wildenthal.[10]

The $S_{jj'}^{Op}$ are the matrix elements between the single-particle states of the model space of the three operators, defined according to

$$S_{jj'}^{Op} = \langle j |||Op(\Delta J, \Delta T)|||j' \rangle$$
$$= [2(2\Delta T + 1)]^{1/2} \langle j ||Op(\Delta J)||j' \rangle \ . \tag{8}$$

We assume that the higher-order corrections to these shell-model expressions can be incorporated into the values of the $S_{jj'}^{Op}$. In the most general formulation each of the five (j,j') elements of the sd-shell space can have an independent correction for a given observable. A useful way to express these corrections is in terms of more general $M1$ and GT operators which include the term

$$p = (8\pi)^{1/2}[Y^{(2)} \otimes s]^{(1)} \ . \tag{9}$$

We choose to work with the particular formulations of the $M1$ and GT single-particle operators defined by the following general expression:

$$Op = g_s[S(d\text{-}d) + S(s\text{-}s)] + g_l L(d\text{-}d) + g_s \delta Op \ , \tag{10}$$

where

$$\delta Op = \delta_s(d\text{-}d)S(d\text{-}d) + \delta_s(s\text{-}s)S(s\text{-}s)$$
$$+ \delta_l L(d\text{-}d) + \delta_p(s\text{-}d)P(s\text{-}d)$$
$$+ \delta_p(d\text{-}d)P(d\text{-}d) \tag{11}$$

and

$$S = \sum_i s_i, \quad L = \sum_i l_i, \quad P = \sum_i p_i \ . \tag{12}$$

The values of the coefficients g and δ depend upon the observables. The g coefficients are obtained from the free-nucleon manifestations of the operator and the δ coefficients characterize the renormalizations which are needed when working within the sd-shell model space. The parentheses $(d\text{-}d)$, $(s\text{-}d)$, and $(s\text{-}s)$ identify the respective pairs of orbits, $l=2$ ($0d_{5/2}$ and $0d_{3/2}$) and $l=0$ ($1s_{1/2}$) which are acted on by the operators. The reduced single-particle matrix elements for the individual operator components s, l, and p are given in Table I.

The term δOp has been multiplied by g_s so that $100\delta_s$ can be regarded as the percentage renormalization of the S matrix element or, alternatively, as the percentage renormalization of the spin g factor g_s; these are equivalent ways of expressing the same result. For the $M1$ operator, $(g_s/g_l) 100\delta_l$ can be regarded as the percentage deviation in the L matrix element or in g_l.

The coefficients $\delta(s\text{-}d)$ and $\delta(s\text{-}s)$ are uniquely proportional to the differences between the free nucleon and empirical values of the $1s_{1/2}\text{-}0d_{3/2}$ and $1s_{1/2}\text{-}1s_{1/2}$ single-particle matrix elements, respectively. The relationships between the remaining three $d\text{-}d$ matrix elements can be expressed concisely in terms of the quantities

$$\delta(j,j') = \langle j ||\delta Op||j' \rangle / \langle j ||s||j' \rangle \ . \tag{13}$$

From Table I, we obtain the general results

$$\delta(++) = \delta_s(l\text{-}l) + 2l\delta_l(l\text{-}l)$$
$$+ [2l/(2l+3)]\delta_p(l\text{-}l) \ ,$$

$$\delta(--) = \delta_s(l\text{-}l) - 2(l+1)\delta_l(l\text{-}l)$$
$$+ [2(l+1)/(2l-1)]\delta_p(l\text{-}l) \ ,$$

$$\delta(+-) = \delta_s(l\text{-}l) - \delta_l(l\text{-}l) - (\tfrac{1}{2})\delta_p(l\text{-}l) \ , \tag{14}$$

where $\delta(++)$ stands for $\delta(l+\frac{1}{2}, l+\frac{1}{2})$, etc. Specifically, for the sd shell $d\text{-}d$ matrix elements

$$\delta(5\text{-}5) = \delta_s(d\text{-}d) + 4\delta_l(d\text{-}d) + (\tfrac{4}{7})\delta_p(d\text{-}d) \ ,$$

$$\delta(3\text{-}3) = \delta_s(d\text{-}d) - 6\delta_l(d\text{-}d) + 2\delta_p(d\text{-}d) \ , \tag{15}$$

$$\delta(5\text{-}3) = \delta_s(d\text{-}d) - \delta_l(d\text{-}d) - (\tfrac{1}{2})\delta_p(d\text{-}d) \ .$$

These relations can be inverted to obtain the general results

TABLE I. Reduced single-particle matrix elements $\langle j||x||j'\rangle$ of the operators $x=s$, l, and p.[a] The matrix elements are obtained by taking the products of the expressions in column G with the respective entries in the columns labeled l, s, and p.

j	j'	G	l	s	p
$l+\frac{1}{2}$	$l+\frac{1}{2}$	$[2(l+1)(2l+3)/(2l+1)]^{1/2}$	l	$\frac{1}{2}$	$l/(2l+3)$
$l-\frac{1}{2}$	$l-\frac{1}{2}$	$[(2l)(2l-1)/(2l+1)]^{1/2}$	$l+1$	$-\frac{1}{2}$	$-(l+1)/(2l-1)$
$l+\frac{1}{2}$	$l-\frac{1}{2}$	$[2(l+1)(l)/(2l+1)]^{1/2}$	1	-1	$\frac{1}{2}$
$l+\frac{1}{2}$	$(l+2)-\frac{1}{2}$	$[2(l+2)(l+1)/(2l+3)]^{1/2}$	0	0	$-3R/2$[b]

[a]Our reduced matrix elements convention is that of Edmonds (Ref. 59) and $\langle j'||x||j\rangle=(-1)^{j-j'}\langle j||x||j'\rangle$.

[b]R is the radial overlap integral. For the $0s$-$1d$ shell $R=-(2/5)^{1/2}$.

$$\delta_s(l\text{-}l)=\frac{(2l+3)(2l+2)\delta(++)+(2l-1)\delta(--)+16l(l+1)\delta(+-)}{6(2l+1)^2} \, ,$$

$$\delta_l(l\text{-}l)=\frac{(2l+3)\delta(++)-(2l-1)\delta(--)-4\delta(+-)}{2(2l+1)^2} \, ,$$

$$\delta_p(l\text{-}l)=\frac{(2l+3)(2l-1)[\delta(++)+\delta(--)-2\delta(+-)]}{3(2l+1)^2} \, .$$

(16)

In particular, for the sd shell d-d matrix elements

$$\delta_s(d\text{-}d)=[14\delta(5\text{-}5)+4\delta(3\text{-}3)+32\delta(5\text{-}3)]/50 \, ,$$

$$\delta_l(d\text{-}d)=[7\delta(5\text{-}5)-3\delta(3\text{-}3)-4\delta(5\text{-}3)]/50 \, , \qquad (17)$$

$$\delta_p(d\text{-}d)=[14\delta(5\text{-}5)+14\delta(3\text{-}3)-28\delta(5\text{-}3)]/50 \, .$$

In Eq. (10) the ISM1 and IVM1 values of g_s and g_l are the free-nucleon "g factors" in the isoscalar and isovector combinations, respectively, and the GT g_s value is consistent with the half-life of the free neutron and the 0^+ to 0^+ pure Fermi decays[7]:

$$g_s(\text{ISM1})=0.880 \, ,$$

$$g_l(\text{ISM1})=0.500 \, ,$$

$$g_s(\text{IVM1})=4.706 \, , \qquad (18)$$

$$g_l(\text{IVM1})=0.500 \, ,$$

$$g_s(\text{GT})=|g_A/g_V|=1.251\pm0.009 \, ,$$

$$g_l(\text{GT})=0 \, .$$

In the textbook definitions of these three operators, the δ coefficients vanish. We use the adjective "free-nucleon" or "free" to refer to these limits of the operators and to the values of single-particle matrix elements and total N-particle shell-model matrix elements which are calculated from them.

For the isoscalar $M1$ moments one can make use of the relation

$$J=\langle i\,|\,S_Z\,|\,i\rangle_{M=J}+\langle i\,|\,L_Z\,|\,i\rangle_{M=J} \qquad (19)$$

to obtain the well-known result[13,14]

$$[\mu(\text{ISM1})-J/2]/0.380$$

$$=\langle i\,|\,S_Z\,|\,i\rangle_{M=J}+(0.880/0.380)\langle i\,|\,\delta Op\,|\,i\rangle_{M=J} \, ,$$

(20)

where the numbers in brackets are

$$g_s(\text{ISM1})/[g_s(\text{ISM1})-g_l(\text{ISM1})] \, .$$

We take the left-hand side of Eq. (20) as the observable for the total (isoscalar) spin contribution $\langle S\rangle$ with an operator of the form of Eq. (10) with

$$g_s(\text{IS})=1$$

and

$$g_l(\text{IS})=0 \, . \qquad (21)$$

Because of this trivial J dependence in the isoscalar moments, defects in the shell-model calculations show up much more clearly in the $\langle S\rangle$ matrix elements than in the isoscalar moments themselves. The very good percentage agreement which appears in the usual comparisons of isoscalar moments with theory[15] stems from this large contribution of a model independent term. For this reason, the experimental error in the isoscalar moment must be rather small (usually at most a few percent) for a meaningful comparison to nuclear-structure theory.[16]

There are, historically, many definitions of these effective operators which differ by various constants. Hence, care must be taken in making comparisons between results given by different authors; we have not attempted to conform here to any particular previous convention.

III. SHELL-MODEL PREDICTIONS AND RESULTS OF THE FITS

Our results are based on the experimental data given in Tables II (ISM1 data) and III (IVM1 and GT data). In

TABLE II. Experimental and theoretical isoscalar moments for sd-shell nuclei.

A	J	T	$[\mu(\text{ISM1})-J/2]/0.380$ Exp[b]	Fit[c]	Free[d]	$\langle S \rangle$[a] $(d\text{-}d)$	$\langle S \rangle$ $(s\text{-}s)$	$\langle L \rangle$ $(d\text{-}d)$	$\langle P \rangle$ $(d\text{-}d)$	$\langle P \rangle$ $(s\text{-}d)$
$T=\frac{1}{2}$ ground state										
17	$\frac{5}{2}$	$\frac{1}{2}$	0.432(2)	0.469	0.500	0.500	0.000	2.000	0.286	0.000
19	$\frac{1}{2}$	$\frac{1}{2}$	0.318(1)	0.376	0.466	0.244	0.223	0.034	−0.001	0.011
21	$\frac{3}{2}$	$\frac{1}{2}$	0.295	0.265	0.303	0.363	−0.059	1.197	0.070	0.007
23	$\frac{3}{2}$	$\frac{1}{2}$		0.242	0.267	0.318	−0.051	1.233	0.064	0.015
25	$\frac{5}{2}$	$\frac{1}{2}$	0.382(2)	0.401	0.399	0.386	0.014	2.102	0.289	−0.018
27	$\frac{5}{2}$	$\frac{1}{2}$	0.376(3)	0.391	0.373	0.332	0.041	2.128	0.286	0.006
29	$\frac{1}{2}$	$\frac{1}{2}$	0.236	0.179	0.131	−0.155	0.286	0.369	0.214	−0.022
31	$\frac{1}{2}$	$\frac{1}{2}$	0.189	0.204	0.161	−0.161	0.322	0.339	0.178	−0.011
33	$\frac{3}{2}$	$\frac{1}{2}$		−0.080	−0.192	−0.183	−0.009	1.691	−0.538	0.089
35	$\frac{3}{2}$	$\frac{1}{2}$	−0.061(3)	−0.071	−0.180	−0.175	−0.005	1.680	−0.569	0.100
37	$\frac{3}{2}$	$\frac{1}{2}$		−0.161	−0.323	−0.323	0.000	1.823	−0.536	−0.013
39	$\frac{3}{2}$	$\frac{1}{2}$	−0.114	−0.149	−0.300	−0.300	0.000	1.800	−0.600	0.000
Other states										
18	5	0	0.921(79)[e]	0.937	1.000	1.000	0.000	4.000	0.571	0.000
22	1	0	0.105(24)	0.150	0.160	0.187	−0.027	0.841	0.089	−0.040
22	3	0	0.647(8)	0.631	0.752	0.821	−0.069	2.249	0.072	0.055
26	5	0		0.863	0.885	0.839	0.046	4.117	0.568	−0.004
30	1	0		0.349	0.269	−0.240	0.509	0.731	0.140	0.206
34	3	0		−0.209	−0.454	−0.434	−0.20	3.454	−1.133	0.138
38	3	0	−0.332(3)	−0.344	−0.689	−0.689	0.000	3.689	−1.109	−0.001
17	$\frac{1}{2}$	$\frac{1}{2}$		0.447	0.500	0.000	0.500	0.000	0.000	0.000
17	$\frac{3}{2}$	$\frac{1}{2}$		−0.187	−0.300	−0.300	0.000	1.800	−0.600	0.000
19	$\frac{5}{2}$	$\frac{1}{2}$	0.483(16)	0.492	0.524	0.471	0.054	1.976	0.236	0.031
21	$\frac{5}{2}$	$\frac{1}{2}$		0.368	0.366	0.391	−0.025	2.135	0.237	−0.014
23	$\frac{5}{2}$	$\frac{1}{2}$		0.337	0.317	0.337	−0.021	2.184	0.234	−0.008
39	$\frac{1}{2}$	$\frac{1}{2}$		0.429	0.500	0.000	0.500	0.000	0.000	0.000
39	$\frac{5}{2}$	$\frac{1}{2}$		0.459	0.500	0.500	0.000	2.000	0.286	0.000
20	2	1	0.609(1)	0.573	0.693	0.615	0.078	1.308	0.067	0.004
24	4	1		0.711	0.766	0.791	−0.025	3.236	0.355	0.025
24	1	1		0.141	0.115	0.076	0.039	0.885	0.195	−0.038
28	3	1		0.566	0.506	0.169	0.337	2.495	0.485	−0.099
32	1	1		−0.109	−0.164	−0.052	−0.112	1.164	−0.424	−0.004
36	2	1	−0.219(1)	−0.191	−0.397	−0.393	−0.004	2.397	−0.747	0.075

[a]$\langle x \rangle = \langle i \mid x_Z \mid i \rangle_{M=J}$.
[b]Experimental values from Refs. 60 and 61. Errors are given in parentheses when they are significant.
[c]Theoretical values obtained with the δ parameters from the $A=18-38$ mass-dependent fit (see Table IV).
[d]Theoretical values obtained with the parameters $\delta_s = \delta_l = \delta_p = 0$.
[e]Not included in the least squares fits because of large experimental error.

TABLE III. Experimental and theoretical isovector magnetic moments and GT matrix elements for sd-shell nuclei.

A	J	T	$\dfrac{\lvert M(\mathrm{GT})\rvert/g_s(\mathrm{GT})}{2[(2J+1)(J+1)/J]^{1/2}}$ Exp[b]	Fit[c]	Free[d]	$\mu(\mathrm{IVM1})/g_s(\mathrm{IVM1})$ Exp[b]	Fit[c]	Free[d]	$\langle S\rangle$[a] (d-d)	$\langle S\rangle$ (s-s)	$\langle L\rangle$ (d-d)	$\langle P\rangle$ (d-d)	$\langle P\rangle$ (s-d)
$T=\frac{1}{2}$ ground states													
17	$\frac{5}{2}$	$\frac{1}{2}$	0.437(1)	0.395	0.500	0.703	0.691	0.713	0.500	0.000	2.000	0.286	0.000
19	$\frac{1}{2}$	$\frac{1}{2}$	0.371	0.378	0.484	−0.480	−0.504	−0.528	−0.280	−0.204	−0.415	−0.023	0.011
21	$\frac{3}{2}$	$\frac{1}{2}$	0.220(1)	0.213	0.281	0.324	0.336	0.359	0.314	−0.033	0.731	0.040	0.008
23	$\frac{3}{2}$	$\frac{1}{2}$	0.169(2)	0.170	0.228		−0.270	−0.291	−0.274	0.046	−0.591	−0.015	−0.061
25	$\frac{5}{2}$	$\frac{1}{2}$	0.272(1)	0.263	0.344	0.478	0.478	0.491	0.325	0.019	1.380	0.236	0.021
27	$\frac{5}{2}$	$\frac{1}{2}$	0.233(2)	0.244	0.313	−0.478	−0.466	−0.466	−0.228	−0.085	−1.436	−0.268	−0.075
29	$\frac{1}{2}$	$\frac{1}{2}$	0.121(3)	0.116	0.135	0.190	0.195	0.170	−0.141	0.276	0.332	0.210	−0.013
31	$\frac{1}{2}$	$\frac{1}{2}$	0.121(2)	0.119	0.141	−0.172	−0.172	−0.151	0.133	−0.274	−0.092	−0.194	0.010
33	$\frac{3}{2}$	$\frac{1}{2}$	0.093(2)	0.095	0.127		0.026	0.005	−0.104	−0.023	1.248	−0.513	0.067
35	$\frac{3}{2}$	$\frac{1}{2}$	0.087(2)	0.093	0.127	−0.020	−0.018	−0.004	0.119	0.008	−1.156	0.453	−0.030
37	$\frac{3}{2}$	$\frac{1}{2}$	0.181(2)	0.173	0.242		−0.091	−0.125	−0.225	0.016	1.097	−0.388	−0.064
39	$\frac{3}{2}$	$\frac{1}{2}$	0.202(2)	0.212	0.300	0.067	0.057	0.109	0.300	0.000	−1.800	0.600	0.000
Other states													
17	$\frac{1}{2}$	$\frac{1}{2}$		0.405	0.500		0.500	0.500	0.000	0.500	0.000	0.000	0.000
17	$\frac{3}{2}$	$\frac{1}{2}$		0.234	0.500		−0.070	−0.109	−0.300	0.000	1.800	−0.600	0.000
19	$\frac{5}{2}$	$\frac{1}{2}$		0.350	0.452	−0.462(1)	−0.444	−0.475	−0.340	−0.112	−0.211	−0.042	−0.044
21	$\frac{5}{2}$	$\frac{1}{2}$		0.251	0.326		0.414	0.432	0.308	0.018	0.994	0.148	−0.010
23	$\frac{5}{2}$	$\frac{1}{2}$		0.184	0.241		−0.311	−0.323	−0.234	−0.007	−0.776	−0.076	−0.070
39	$\frac{1}{2}$	$\frac{1}{2}$		0.373	0.500		−0.499	−0.500	0.000	−0.500	0.000	0.000	0.000
39	$\frac{5}{2}$	$\frac{1}{2}$		0.359	0.500		−0.684	−0.713	−0.500	0.000	−2.000	−0.286	0.000
20	2	1				−0.183	−0.162	−0.173	−0.055	−0.145	0.255	0.049	0.066
24	4	1					0.130	0.120	0.009	0.040	0.666	0.199	−0.061
24	1	1					0.516	0.541	0.422	−0.022	1.334	0.163	0.068
28	3	1					−0.271	−0.294	−0.400	0.239	−1.257	−0.122	−0.149
32	1	1					0.151	0.121	−0.133	0.139	1.080	−0.352	0.293
36	2	1				−0.078	−0.082	−0.089	−0.071	−0.009	−0.081	0.053	−0.111

[a]$\langle x\rangle = \langle i\,|\,x_z\tau_z\,|\,i\rangle_{M=J,T_z=T}$.

[b]Experimental values from Refs. 60 and 61. Errors are given in parentheses when they are significant.

[c]Theoretical values obtained with the δ parameters from the $A=18-38$ mass-dependent fit (see Table IV).

[d]Theoretical values obtained with the parameters $\delta_s=\delta_l=\delta_p=0$.

TABLE IV. Comparison between theoretical and empirical values of the parameters δ_s, δ_l, and δ_p. The theoretical values are taken from the calculations of Towner and Khanna (Ref. 1), details of which are given in Table V.

δ_s (d-d)	δ_s (s-s)	δ_l (d-d)	δ_p (d-d)+(s-d)	rms[a]	
Isoscalar S[b]					
−0.330		0.048	0		$A=17$ and 39, no mass dependence, $\delta_p=0$
−0.27(2)	−0.06(7)	0.045(5)	0	0.0359	$A=17-39$, no mass dependence, $\delta_p=0$
−0.30(5)	−0.08(8)	0.049(9)	0.03(5)	0.0370	$A=17-39$, no mass dependence
−0.31(5)	−0.11(9)	0.047(9)	0.06(6)	0.0371	$A=17-39$, $(A/28)^{0.35}$ mass dependence
−0.30(5)	−0.10(9)	0.051(10)	0.05(6)	0.0385	$A=18-38$, no mass dependence
−0.32(5)	−0.13(9)	0.050(10)	0.08(6)	0.0381	$A=18-38$, $(A/28)^{0.35}$ mass dependence
−0.293	−0.300	0.024	−0.002		Average of $A=16$ and 40 theory from Table V
Isovector $M1$					
−0.068		0.012	0		$A=17$, and 39, no mass dependence, $\delta_p=0$
−0.087(18)	0.015(32)	0.012(5)	0	0.0150	$A=17-39$, no mass dependence, $\delta_p=0$
−0.103(25)	0.003(34)	0.014(5)	0.021(23)	0.0152	$A=17-39$, no mass dependence
−0.110(27)	−0.006(37)	0.013(5)	0.028(24)	0.0151	$A=17-39$, $(A/28)^{0.35}$ mass dependence
−0.108(30)	0.008(39)	0.013(8)	0.016(30)	0.0170	$A=18-38$ no mass dependence
−0.116(33)	−0.001(42)	0.013(8)	0.022(30)	0.0169	$A=18-38$, $(A/28)^{0.35}$ mass dependence
−0.090	−0.108	0.011	0.042		Average of $A=16$ and 40 theory from Table V
Isovector GT					
−0.206		0.020	0		$A=17$ and 39, no mass dependence, $\delta_p=0$
−0.234(18)	−0.209(35)	0.011(4)	0	0.0156	$A=17-39$, no mass dependence, $\delta_p=0$
−0.243(34)	−0.218(47)	0.012(6)	0.001(29)	0.0164	$A=17-39$, no mass dependence
−0.271(32)	−0.242(43)	0.010(5)	0.028(27)	0.0140	$A=17-39$, $(A/28)^{0.35}$ mass dependence
−0.246(16)	−0.197(21)	0.003(3)	−0.004(13)	0.0073	$A=18-38$, no mass dependence
−0.276(20)	−0.227(26)	0.004(4)	0.018(16)	0.0083	$A=18-38$, $(A/28)^{0.35}$ mass dependence
−0.181	−0.196	0.004	0.022		Average of $A=16$ and 40 theory from Table V

[a]rms deviation for quantities tabulated in Tables II and III.
[b]$\delta(ISM1)=(0.380/0.880)\delta(IS)$.

these tables the data are compared with the predictions obtained by combining the shell-model $D_{jj'}$ with the free-nucleon values of the $S_{jj'}^{Op}$ and with the values of the $S_{jj'}^{Op}$ obtained in our "final" fit. The various fits will be discussed in detail below. The δ parameters obtained from these fits are presented in Table IV in comparison with the calculations of Towner and Khanna.[1] This comparison will be discussed in Sec. V.

In Table II, as noted above, we express the isoscalar moments in terms of the isoscalar spin (IS) expectation value

[see Eq. (20)]. The comparison of the isovector observables is facilitated by dividing the IVM1 moments by $g_s(IVM1)$ and by dividing the $T=\frac{1}{2}\rightarrow\frac{1}{2}$ GT matrix elements by the factor

$$2g_s(GT)\times[(2J+1)(J+1)/J]^{1/2},$$

as has been done in Table III. The theoretical values for these divided isovector quantities as well as the isoscalar spin expectation values are all given by

$$\langle S_Z\tau\rangle+(g_l/g_s)\langle L_Z\tau\rangle+\langle\delta Op\tau\rangle=\langle S_Z\tau\rangle(d\text{-}d)+\langle S_Z\tau\rangle(s\text{-}s)+(g_l/g_s)\langle L_Z\tau\rangle(d\text{-}d)$$
$$+\delta_s(d\text{-}d)\langle S_Z\tau\rangle(d\text{-}d)+\delta_s(s\text{-}s)\langle S_Z\tau\rangle(s\text{-}s)+\delta_l(d\text{-}d)\langle L_Z\tau\rangle(d\text{-}d)$$
$$+\delta_p(d\text{-}d)\langle P_Z\tau\rangle(d\text{-}d)+s_p(s\text{-}d)\langle P_Z\tau\rangle(s\text{-}d),\tag{22}$$

where $\tau=1$ for the IS matrix elements and $\tau=\tau_Z$ for the IVM1 and GT matrix elements. The quantity g_l/g_s is equal to 0, 0.106, and 0 for IS, IVM1, and GT, respectively. The five sd-shell matrix elements involving the S, L, and P operators are listed in Tables II and III for the various AJT states of our data set. The single-particle values of $\langle s_Z\rangle$ are particularly simple: $\frac{1}{2}$ for $j=l+\frac{1}{2}$ orbits and $(-\frac{1}{2})+1/(2l+1)$ for $j=l-\frac{1}{2}$ orbits.

Within the isovector category, the $M1$ and GT matrix

elements both involve the same shell-model expectation values of the S, L, and P operators. The total GT and IVM1 shell-model matrix elements differ in zeroth order in that the coefficients of the L term are different. This term appears only to order δ_l in the GT expression. We will emphasize here the importance of the quantitative dissimilarities between such matrix elements which arise because of the non-negligible contributions of the l term in some cases and, more fundamentally, because of intrinsic

differences between some of the higher-order corrections to weak and to electromagnetic processes.

The comparison between experiment and theory for the $T = \frac{1}{2}$ states is presented graphically in Fig. 1. In the top panels of Fig. 1 we plot the absolute values of the results as given in Tables II and III. In the middle panels the same points are plotted in a representation in which only the S portions of the theoretical values are shown and in which the theoretical values (fitted parameters) of L and P have been subtracted from the corresponding experimental values. In the bottom panels, the ratios of experiment to theory for these points are shown, with the L and P contributions subtracted as in the middle panels.

The experimental data we consider are generally known to much greater precision than can be calculated, and hence, they were given equal weight in the fits. The uncertainties we assign to our extracted correction parameters are determined in the usual way, by assigning a fictitious error to the experimental data such as to give a reduced chi-square of unity.

We initially made fits to the data in which all five of the δ parameters in Eq. (11) were allowed to vary. By an order of magnitude, the least well determined parameter was $\delta_p(s\text{-}d)$. This could be expected from the small contribution that the operator $P(s\text{-}d)$ makes to the total matrix elements in Tables II and III. In the calculations of Towner and Khanna,[1] the values of $\delta_p(d\text{-}d)$ and $\delta_p(s\text{-}d)$ are nearly equal (see Table V). With these motivations, we reduced the fits to ones in which only four, rather than five, parameters are varied by combining the $P(d\text{-}d)$ and $P(s\text{-}d)$ terms into a single "P" term:

$$\delta_p P = \delta_p(d\text{-}d)P(d\text{-}d) + \delta_p(s\text{-}d)P(s\text{-}d) . \quad (23)$$

The rms deviations obtained in the four-parameter fits (see Table IV) are nearly the same as those obtained in three-parameter fits in which the values of δ_p are constrained to be zero. This is not because the matrix elements of the operator P are small but because the values of the parameters δ_p are in fact determined by the data to be nearly zero. Even though the uncertainties in the
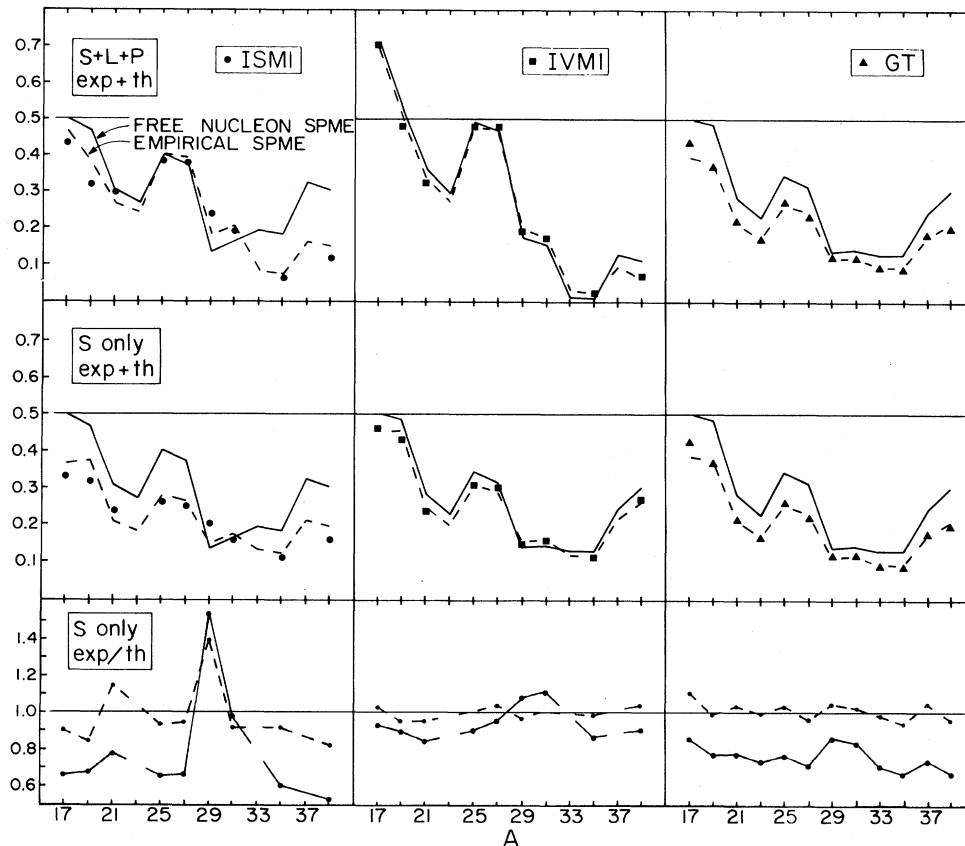

FIG. 1. Comparisons of normalized experimental values of the isoscalar and isovector magnetic dipole moments (ISM1 and IVM1, respectively) and Gamow-Teller beta-decay matrix elements (GT) for the mirror ground states of $A = 17-39$ nuclei with predictions of mixed-configuration sd-shell model wave functions. The solid lines are obtained with single-particle matrix elements set to the free-nucleon values, while the dashed lines are obtained with single-particle matrix elements set to the "final fit" values of the present study. The normalization functions are defined in Tables II and III. The top three panels show the renormalized experimental and both free-nucleon and final fit theoretical values. The middle three panels show only the spin components of these matrix elements. The "experimental" values are obtained by subtracting the final fit L and P theoretical values from the experimental values shown in the top panels. The bottom three panels show the ratios of experimental to theoretical values for the spin components of these matrix elements as they are defined for the middle three panels.

TABLE V. Details of the theoretical calculations for the δ parameters.

	δ_s (d-d)	δ_s (s-s)	δ_l (d-d)	δ_p (d-d)	δ_p (s-d)	
Isoscalar S						
	−0.229	−0.247	0.026	−0.004	−0.005	$A=16$ theory from Towner and Khanna (Ref. 1)
	−0.358	−0.352	0.021	−0.001	0.000	$A=40$ theory from Towner and Khanna
Details of $A=40$ theory from Towner and Khanna						
(1)	−0.121	−0.105	0.011	−0.004	−0.004	$2\hbar w$ configuration mixing
(2)	−0.287	−0.287	0.013	0.001	−0.001	$>2\hbar w$ configuration mixing
(3)	0	0	0	0	0	Isobar currents, RPA direct
(4)	0	0	0	0	0	Isobar currents, RPA exchange
(5)	0.000	−0.003	0.000	−0.003	−0.001	Isobar currents, higher order
(6)	0.021	0.016	0	0.006	0.008	Mesonic exchange currents, zeroth order
(7)	0.000	0.003	0.000	0.003	0.004	Mesonic exchange currents, RPA
(8)	0.029	0.026	0.000	−0.004	−0.006	Mesonic exchange currents, CP
Isovector $M1$						
	−0.079	−0.103	0.0115	0.0455	0.0464	$A=16$ theory from Towner and Khanna (Ref. 1)
	−0.101	−0.112	0.0104	0.0384	0.0377	$A=40$ theory from Towner and Khanna
Details of $A=40$ theory from Towner and Khanna						
(1)	−0.065	−0.058	−0.0225	0.0104	0.0094	$2\hbar w$ configuration mixing
(2)	−0.115	−0.125	−0.0261	0.0018	−0.0078	$>2\hbar w$ configuration mixing
(3)	−0.081	−0.085	0.0002	0.0155	0.0221	Isobar currents, RPA direct
(4)	0.042	0.045	0.0000	0.0001	0.0031	Isobar currents, RPA exchange
(5)	0.001	−0.002	−0.0002	0.0094	0.0122	Isobar currents, higher order
(6)	0.053	0.051	0.0363	−0.0161	−0.0214	Mesonic exchange currents, zeroth order
(7)	0.002	0.003	−0.0004	−0.0003	0.0011	Mesonic exchange currents, RPA
(8)	0.061	0.059	0.0232	0.0176	0.0190	Mesonic exchange currents, CP
Isovector GT						
	−0.151	−0.167	0.005	0.0164	0.0276	$A=16$ theory from Towner and Khanna (Ref. 1)
	−0.212	−0.224	0.004	0.0162	0.0259	$A=40$ theory from Towner and Khanna
Details of $A=40$ theory from Towner and Khanna						
(1)	−0.063	−0.055	0.002	0.0065	0.0076	$2\hbar w$ configuration mixing
(2)	−0.113	−0.119	0.001	0.0010	0.0028	$>2\hbar w$ configuration mixing
(3)	−0.081	−0.085	0.000	0.0156	0.0221	Isobar currents, RPA direct
(4)	0.042	0.045	0.000	0.0002	0.0031	Isobar currents, RPA exchange
(5)	0.002	−0.001	0.000	0.0102	0.0146	Isobar currents, higher order
(6)	−0.010	−0.010	0	−0.0114	−0.0167	Mesonic exchange currents, zeroth order
(7)	0.002	0.003	0	−0.0013	−0.0015	Mesonic exchange currents, RPA
(8)	0.026	0.017	0.000	0.0049	0.0071	Mesonic exchange currents, CP
(9)	−0.019	−0.019	0	−0.0092	−0.0131	Relativistic

varied parameters are smaller in the fits in which δ_p is constrained to be zero, there is no theoretical reason why δ_p should be exactly zero. The remaining discussion will be concerned with the results of the four-parameter fits.

The final results were obtained by fitting the $A=18-38$ data with mass-dependent δ parameters of the form

$$\delta(A) = \delta_0 (A/28)^X . \qquad (24)$$

Even though the fitted parameter values depend somewhat on the power X, the rms deviation changes little over the range $X=0$ to 1 due to a correlation between X and the δ parameters. Thus, we have chosen a value of $X=0.35$ based on the calculations of Towner and Khanna.[1] This is based on their results for δ_s given in Table V for $A=16$ and 40 which give for the d orbit $X=0.49$, 0.28, and 0.37 for ISM1, IVM1, and GT, respectively, and for the s orbit

$X=0.39$, 0.09, and 0.32, respectively. Comparisons of the parameter values obtained with $X=0$ and 0.35 are made in Table IV.

The rationale for omitting $A=17$ and 39 from the final fit was to determine the extent to which the observables for the single-particle states in these nuclei are consistent with what can be extracted from the $A=18-38$ "multiparticle" states. The parameter values extracted from both $A=17-39$ and $A=18-38$ fits are compared in Table IV. Based on a comparison of the rms deviations, we conclude that for $M1$ observables, the $A=17$ and 39 data are quite consistent with $A=18-38$. However, for GT observables they are less consistent, with the rms deviation becoming a factor of 2 larger when the $A=17$ and 39 data are added to the $A=18-38$ data.

IV. DISCUSSION OF CALCULATED AND MEASURED VALUES OF OBSERVABLES

A. Isoscalar magnetic dipole moments

The experimental isoscalar magnetic moment data are compared with both the free-nucleon and empirically corrected shell-model predictions in Table II. The free-nucleon predictions have magnitudes larger than the experimental values at both the beginning ($d_{5/2}$-like) and end ($d_{3/2}$-like) of the $A=17-39$ region and magnitudes smaller than experiment in the $A=30$ ($s_{1/2}$-like) region. The empirically corrected predictions reproduce experiment much better than do the free-nucleon values. However, the level of disagreement between the fitted and experimental values is still considerably higher than that which we find for the IVM1 and GT phenomena.

From the S, L, and P matrix elements given in Table II the essential features of the predicted structures of the states can be inferred. The generic similarities between the Hamiltonian-independent, single-hole $0d_{3/2}$ wave function for the $\frac{3}{2}^+$ ground state of $A=39$ and those of the $0d_{3/2}$-dominated $\frac{3}{2}^+$ ground states of $A=33$, 35, and 37 are evident from these decompositions, as are the analogous similarities between the single-particle $0d_{5/2}$ wave function of the $\frac{5}{2}^+$ ground state of $A=17$ and those of the $\frac{5}{2}^+$ states in $A=19$, 21, 23, 25, and 27. The dominant role of the $0d_{5/2}$ orbit in the wave functions of the $\frac{3}{2}^+$ ground states of $A=21$ and 23 is revealed by the very different relationship of $\langle L \rangle$ to $\langle S \rangle$ they evidence compared to that of the $\frac{3}{2}^+$ states of $A=33$, 35, 37, and 39.

The $\frac{1}{2}^+$ ground states of $A=29$ and 31 are predicted to have similar structures. In both wave functions there is a significant contribution from $\langle L \rangle$ and the $l=2$ and 0 components of $\langle S \rangle$ have opposite signs. These wave functions have the signature of a dominant $1s_{1/2}$ character, with the most important admixtures being of $0d_{3/2}$ origin. The $A=19$ $\frac{1}{2}^+$ ground state, on the other hand, shows a completely different structure, in which the contribution of $\langle L \rangle$ is negligible and the $l=2$ and 0 components of $\langle S \rangle$ have the same sign.

Several of the doubly-odd $T=0$ states are seen to be simply related to even-odd $T=\frac{1}{2}$ states. The 3^+ states of $A=38$ and 34 can be grouped with the $\frac{3}{2}^+$ states of $A=33$, 35, 37, and 39. The 1^+ state of $A=30$ can be

grouped with the $\frac{1}{2}^+$ states of $A=29$ and 31 and the 5^+ states of $A=18$ and 26 can be grouped with the $\frac{5}{2}^+$ states of $A=17-27$.

The values of $\delta_s(\text{ISM}1,s\text{-}s)$ and $\delta_p(\text{ISM}1)$ are not well determined by the available data. The value obtained for $\delta_s(\text{ISM}1,s\text{-}s)$ has the same sign but only one-third the magnitude of the value of $\delta_s(\text{ISM}1,d\text{-}d)$ and the uncertainty associated with this value of $\delta_s(\text{ISM}1,s\text{-}s)$ is as large as the value itself. The value obtained for $\delta_p(\text{ISM}1)$ is small and positive and, with its uncertainty, is consistent with zero.

The lack of precision with which the correction term $\delta_s(\text{ISM}1,s\text{-}s)$ is determined by the present analysis reflects the relationships of the free-nucleon shell-model predictions for the $\frac{1}{2}^+$ states of $A=19$, 29, and 31 to the experimental values. The $A=19$ prediction is too large and the $A=29$ and 31 predictions too small. Hence, to the degree that the shell-model predictions are dominated by their $\langle S \rangle(s\text{-}s)$ components, a correction which improves agreement for $A=19$ tends to cause a deterioration of the agreement for $A=29$ and 31, and vice versa. These three are the only cases in which the $1s_{1/2}$ orbit is predicted to be important and for which measured values exist. Other states in which this orbit is predicted to play a dominant role are the 3^+, $T=1$ state of $A=28$, the 1^+, $T=0$ state of $A=30$ and, to a lesser degree, the 1^+, $T=1$ state of $A=32$. Experimental measurements in these three additional cases should significantly improve the precision with which the correction term $\delta_s(\text{ISM}1,s\text{-}s)$ is determined.

The fundamental problem in determining this correction, however, is associated with the reliability of the shell-model expectation values. All of the available and potentially available data which bear on this term come from states which are predicted to have richly complicated structures. This can be inferred from a comparison of predicted expectation values for the $\frac{1}{2}^+$ states to those of the pure $1s_{1/2}$ single-particle state (see the entry for $A=17$, $J=\frac{1}{2}$ in Tables II and III). Hence, relative to the determination of the $0d_{3/2}$ and $0d_{5/2}$ corrections, for which there are data from pure (in the model context) single-particle states as well as from a succession of fair approximations to single-particle structure, the determination of the $1s_{1/2}$ correction depends completely upon the details of the specific shell-model wave functions used in the analysis. While additional experimental data will help in allowing the analysis to average over isolated defects in these wave functions, the fact that all the feasible examples except that for $A=19$ are clustered in the $A=28-32$ region means that a systematic defect in the predicted structures of this region will propagate into the extracted value of $\delta_s(\text{ISM}1,s\text{-}s)$.

B. Isovector magnetic dipole moments

The experimental isovector magnetic-moment values are compared with both the free-nucleon and empirically corrected shell-model predictions in Table III. The free-nucleon predictions are close to the measured values of the $A=17$, 19, 25, and 27 $J^\pi=\frac{5}{2}^+$ states, even though the magnitudes of these moments decrease progressively as A increases (see Fig. 1). This experimentally observed

quenching with increasing A (see also Fig. 1) emerges from the shell-model predictions as a consequence of the A-dependent configuration mixing induced by the Hamiltonian. Hence, it does not constitute evidence of the need for A-dependent, higher-order corrections to the description of the isovector $M1$ process. From the decompositions of the isovector shell-model expectation values presented in Table III we see that the quenching can be associated principally with a diminution of $\langle L \rangle$ in the multiparticle systems relative to the single-particle value. The 2^+, $T=1$ state of $A=20$ and the $\frac{3}{2}^+$, $T=\frac{1}{2}$ state of $A=21$ are dominated by the $d_{5/2}$ orbit and the relationships between the observed and calculated values of their isovector moments are consistent with those of the $\frac{5}{2}^+$ states.

The small negative values of μ(IVM1) observed for the $\frac{3}{2}^+$ states of $A=35$ and 39 are less negative than the small values calculated for them with the free-nucleon assumption, the overall smallness of the magnitudes stemming from the cancellation of the $\langle L \rangle$ and $\langle S \rangle$ contributions to the $d_{3/2}$ moment. The decompositions for the $\frac{3}{2}^+$ states show that the expectation values obtained from the multiparticle wave functions deviate markedly from the single-particle values of both $\langle S \rangle$ and $\langle L \rangle$. In addition, these deviations are seen to vary significantly with A. The $A=35$ values, both observed and calculated, are at least three times smaller than their $A=39$ counterparts. The only other experimental value for a $d_{3/2}$-dominated state is that of the 2^+, $T=1$ state in $A=36$. However, the small value of the isovector moment for this state stems from the dominance of the $d_{3/2}$ orbit in its wave function and particle-hole symmetry, which requires that the isovector moment for the (half-shell) $(d_{3/2})^4$ configuration equal zero. The best chances to obtain the needed augmentation of experimental information on the behavior of the $d_{3/2}$ orbit in the context of isovector $M1$ phenomena lie in measurements of the $A=33$ and 37 ground-state moments.

Of the $\frac{1}{2}^+$ states with measured isovector moments, which occur in $A=19$, 29, and 31, the values for $A=19$, both experimental and calculated, are close to the single-particle value for the $s_{1/2}$ orbit. The magnitudes of the $A=29$ and 31 values are more than a factor of 2 smaller. The shell-model decompositions suggest that these values of the moments are misleading insofar as the structures of the states are concerned, however. The predicted $A=19$ value is seen to be dominated by $l=2$ contributions and the contributions of the $l=0$ orbit are larger in the $A=29$ and 31 cases than in $A=19$. In none of these wave functions is the $l=0$ contribution strongly dominant, however, and this makes the extraction of the correction term δ_s(IVM1,s-s) difficult. In each of these three examples, the $l=2$ contributions are both very important and, moreover, very different in each state. The only other state for which the $l=0$ contribution is significant and for which experimental data exist is the 2^+, $T=1$ state of $A=20$.

The free-nucleon shell-model predictions for these four cases do not appear to have any systematic relationship with the experimental values. The free-nucleon value is 10% too large for $A=19$ and 5—10% too small for

$A=20$, 29, and 31. These results for the isovector values of $1s_{1/2}$-dominated states are reminiscent of those obtained for the isoscalar values of these states. Unlike the results for the isoscalar moments, however, the correction terms δ(IVM1) yield values of the isovector moments which are in significantly better agreement with experiment than are the free-nucleon values. The shell-model decompositions suggest that experimental measurements of the 3^+, $T=1$ state of $A=28$ and the 1^+, $T=1$ state of $A=32$, respectively, would provide further information on the behavior of the $1s_{1/2}$ orbit, but, as with the presently available data, the contributions to their moments of the $l=2$ orbits are of comparable importance to that of the $l=0$ orbit. Again, we add the cautionary note that the multiparticle shell-model predictions are more important to the analysis of the $1s_{1/2}$ orbit than of the $0d_{5/2}$ and $0d_{3/2}$ orbits. Defects in the shell-model results for the region $A=28-32$ will correspondingly vitiate conclusions drawn from the present method of analysis.

C. Gamow-Teller beta decay matrix elements

The remaining area of experimental information we consider in this study is comprised of the Gamow-Teller beta decays between the $T=\frac{1}{2}$ mirror ground states. The shell-model expectation values presented in Table III for these states are the basis for our theoretical predictions for the Gamow-Teller matrix elements just as they were for the IVM1 matrix elements. The critical change introduced in calculating the GT rather than the IVM1 matrix elements from these expectation values is that the $\langle L \rangle$ term contributes only through the higher-order correction term δ_l(GT,d-d) rather than in first order via the coefficient g_l. Hence, to lowest order, the GT matrix elements are functions only of the spin expectation values.

We see from Table III that the free-nucleon shell-model predictions of M(GT), which are functions of $\langle S \rangle$(s-s) and $\langle S \rangle$(d-d) alone, have a quite different relationship with the corresponding experimental values than do the analogous predictions for μ(IVM1) with the experimental μ(IVM1) values. This relationship is quite simply characterized in that the theoretical predictions are too large, by factors ranging from about 1.2 near $A=17$ to about 1.5 near $A=39$ (see Fig. 1). The A-dependent corrections δ_s(GT,s-s) and δ_s(GT,d-d) suffice to bring the $A=19-37$ theoretical values into uniform close agreement with the data. The same (d-d) term also brings the $A=39$ single-particle value into close agreement with experiment but leaves a discrepancy for $A=17$ which, while small, still dominates the rms deviation between the shell-model predictions with higher-order corrections and experiment.

V. COMPARISONS WITH CALCULATIONS OF HIGHER-ORDER CORRECTIONS

We now attempt to relate our empirical values of the correction terms δ to corrections calculated to arise from nuclear configuration mixing outside the sd shell (CM), from isobar currents (IC's), mesonic-exchange currents (MEC's), and relativistic effects (RE's). The most recent

and complete theoretical work in this area for the *sd* shell has been carried out by Towner and Khanna.[1] Previous work in this field is summarized and referenced by Towner and Khanna, and our general introductory remarks here will be brief.

The limitations associated with considering the $M1$ operators in terms of only nucleonic degrees of freedom have been long recognized.[17-20] The inclusion of non-nucleonic effects has become a standard (but not unambiguous) part of more recent $M1$ and GT effective operator calculations.[21-23,4,3,24] These non-nucleonic degrees of freedom are generically referred to as "mesonic-exchange corrections." In recent years much attention has been given to the particular corrections which arises from the excitation of one or more of the nucleons into the resonant $\Delta(1232)$ isobar state.[25-37] For this reason we will consider the IC's separately and refer to all other non-nucleonic degrees of freedom as MEC's. It is important to note that, since the IC corrections are calculated nonrelativistically, the IC correction to the *s*-τ operator is the same for both IVM1 and (IV)GT observables; in our notation

$$\delta_s(\text{IC,IVM1}) = \delta_s(\text{IC,GT}) .$$

However, most of the MEC corrections must be calculated from relativistic Feynman diagrams and, hence, these corrections depend on whether the operator is vector (as for the $M1$) or axial vector (as for the GT).[20,1] It turns out that theoretically the MEC corrections are much larger for the $M1$ operator than for the GT operator; in our notation, $|\delta_s(\text{MEC,IVM1})| \gg |\delta_s(\text{MEC,GT})|$.

One must also consider the corrections to the $M1$ and GT operators which arise from nuclear configuration mixing (CM) beyond our assumed closed-shell configurations for ^{16}O and ^{40}Ca. There are no first-order ($\Delta E = 2\hbar\omega$ 1p-1h) core-polarization corrections, since the l and s operators cannot excite particles into different orbital states. (Of course, within the *sd* shell, our model wave functions explicitly take account of the mixing between the $0d_{5/2}$ and $0d_{3/2}$ spin-orbit partners.) Second-order calculations ($\Delta E \geq 2\hbar\omega$ 2p-2h) have been carried out for some time,[38-41] but it has been discovered only rather recently that these corrections become very large when intermediate states up to about $12\hbar\omega$ are included.[2,3,1] The tensor interaction is responsible for the importance of these highly excited intermediate states. Since these are nonrelativistic calculations,

$$\delta_s(\text{CM,IVM1}) = \delta_s(\text{CM,GT})$$

in the absence of the zeroth-order $M1$ L operator. Even with the inclusion of the L operator this is still a good approximation (see Table V).

In addition to the above corrections, one could consider, for example, local state-dependent 4p-4h CM corrections. Indeed, many of the lowest excited states of ^{16}O and ^{40}Ca are predominantly 4p-4h in nature. This type of CM has been examined in the case of $A=39$.[25,42,3] Although we should not ignore this type of CM, its importance is thought to decrease away from shell closures as the formation of four-particle cluster configurations across the closed shells becomes blocked by the increasing numbers

of particle or holes. Since our fits do not include the $A=17$ and 39 data, the difference between our predictions for these data based on the corrections from the $A=18-38$ fit and the experimental values (see Tables II and III) might be taken as an indication of the size of the 4p-4h CM effects.

Finally we mention the RE corrections to the GT operator[43-45] which have been included in the Towner and Khanna calculations. The relativistic corrections for the $M1$ operator are of order $(1/M)^3$ (where M is the nucleon mass) and, for consistency, have been ignored, since all other MEC's and relativistic corrections have been calculated only to order $(1/M)^2$.[1]

In Table V, the individual contributions to the δ parameters from all of the above effects are given from the $A=40$ calculations of Towner and Khanna.[1,46] The total values for both the $A=16$ and 40 calculations are also given in Table V. The average of the totals for $A=16$ and 40 are compared to our empirical values in Table IV.

There is considerable controversy over the relative importance of the IC and CM corrections in the quenching of the GT matrix elements.[47,1] Part of this controversy centers around what should be used for the interaction between nucleons and isobars in nuclei. Values of δ_s and δ_p obtained with the interactions used by Oset and Rho[28] and Lawson[37] are compared with the results of Towner and Khanna in Table VI.

In the following sections we will discuss some individual points about the comparisons made in Tables IV–VI and in Fig. 1.

A. Isoscalar $M1$ corrections

The first-order and random-phase approximation (RPA) isobar current diagrams do not contribute to the isoscalar moments since the operator must flip the isospin in going between the nucleon and the delta isobar. (For analogous reasons, the π-exchange current contributes only to the isovector moments.) This leaves the short-range ρ-π-γ and ω-π-γ currents as the most important isoscalar MEC contributions. There are two approaches to these MEC calculations in the literature. In one approach they are connected with the velocity dependence of the nuclear interaction, in particular with the spin-orbit term. In this case the method of minimal substitution $p \rightarrow p - (e/c)A$ can be used to deduce a two-body isoscalar magnetic-moment operator[48,49,18] which, when averaged over the closed shells, gives an effective one-body operator. Raman *et al.*[50] obtained with this method (using the Hamada-Johnston potential) $\delta_s(\text{IS,MEC}) = -0.050$ for the d orbit at $A=40$. In the other approach, these correction terms can be obtained from a microscopic calculation. Towner and Khanna (who include also the two π exchange) obtain for the d orbit (see Table V) $\delta_s(\text{IS,MEC}) = 0.050$ for $A=40$. Hyuga *et al.*[4] in a similar calculation obtain the value 0.034 for $A=40$. Our comparisons and conclusions will be based on the microscopic results of Towner and Khanna. However, we note that these conclusions will not be firm until the MEC corrections are better understood.

From Table V it is seen that in the Towner-Khanna cal-

TABLE VI. Comparisons between various isobar-current calculations.

A	$l-l'$	δ_s	δ_p	Order[a]	Interaction[b]	Reference
16	p-p	−0.143	0.021	RPA	OR	Oset and Rho (Ref. 28)[c]
		−0.110	0.015	RPA(D)	TK without FF	Towner and Khanna (Ref. 1)
		−0.027	0.019	RPA	TK without FF	Towner and Khanna (Ref. 1)
		−0.022	0.022	RPA	TK with FF	Towner and Khanna (Ref. 1)
		−0.018	0.029	RPA + CP	TK with FF	Towner and Khanna (Ref. 1)
		−0.025	0.032	1st	SP	Lawson (Ref. 37)[d]
16	d-d	−0.100	0.027	RPA	OR	Oset and Rho (Ref. 28)[c]
		−0.079	0.019	RPA(D)	TK without FF	Towner and Khanna (Ref. 1)
		−0.036	0.023	RPA	TK without FF	Towner and Khanna (Ref. 1)
		−0.028	0.025	RPA	TK with FF	Towner and Khanna (Ref. 1)
		−0.027	0.033	RPA + CP	TK with FF	Towner and Khanna (Ref. 1)
		−0.023	0.031	1st	SP	Lawson (Ref. 37)[d]
40	d-d	−0.151	0.016	RPA	OR	Oset and Rho (Ref. 28)[c]
		−0.136	0.014	RPA(D)	TK without FF	Towner and Khanna (Ref. 1)
		−0.047	0.012	RPA	TK without FF	Towner and Khanna (Ref. 1)
		−0.039	0.016	RPA	TK with FF	Towner and Khanna (Ref. 1)
		−0.037	0.026	RPA + CP	TK with FF	Towner and Khanna (Ref. 1)
		−0.034	0.024	1st	SP	Lawson (Ref. 37)[d]

[a]The orders are denoted by: "1st" for the 1st-order isobar-nucleon-hole calculation, "RPA" for the isobar-nucleon-hole calculation in the random-phase approximation, and "RPA + CP" includes on top of the RPA series higher order nuclear core-polarization corrections (the row labeled 5 in Table V). All calculations include both direct and exchange terms either implicitly (OR) or explicitly (TK and SP) except the calculation labeled RPA(D) which is only the direct contribution.

[b]The interactions are denoted by: "OR" for the Oset-Rho interaction with $g'_\Delta = 0.6$, "TK" for the Towner-Khanna interaction, and "SP" for the Smith-Pandharipande interaction (Ref. 62). All calculations include the effects of short range correlations either implicitly (OR) or explicitly (TK and SP). In addition, Towner and Khanna included explicit nucleon form factor corrections (FF) in their calculation. For comparison their results without the FF corrections (Ref. 46) are also given.

[c]The breakdown of the Oset results into δ_s and δ_p was given by Towner (Ref. 46).

[d]In order to compare with calculations of Towner and Khanna based on the quark model for the $\pi\Delta N$ coupling constant, the results given by Lawson are multiplied by 0.613 (Ref. 37).

culations the configuration-mixing (CM) correction is the most important mechanism for quenching the isoscalar spin matrix elements. The Towner-Khanna results for CM are similar to those of Shimizu, Ichimura, and Arima.[2] The theoretical values for δ_s(IS,d-d) are in good agreement with our empirical values (Table IV). The theoretical values for δ_s(IS,s-s) are similar to the δ_s(IS,d-d) values but our empirical values of δ_s(IS,s-s) are only one-third as large. As mentioned in Sec. IV A, the empirical value extracted for δ_s(IS,s-s) is very sensitive to the details of the configuration mixing in the sd-shell wave functions for $A=29$ and 31. For this reason we do not attach too much significance to a discrepancy of this absolute magnitude.

We take the level of agreement obtained between the empirical and theoretical values of δ_s(IS,d-d) as an indication that the basic ingredients of the CM calculations are correct. Less than half of the theoretical values of δ_s(IS) comes from the $2\hbar\omega$ CM (see Table V). It can be shown[1] that, since the isoscalar $M1$ operator commutes with the central interaction, only second-order CM induced by noncentral interactions contributes to δ_s(IS). These points illustrate the importance of the tensor force.

The empirical value of -0.05 ± 0.01 we obtain for δ_l(IS,d-d) is twice as large as the value obtained in the Towner-Khanna calculation. Our empirical value for δ_p(IS) is zero within its uncertainty and is in agreement with small Towner-Khanna values. We believe the discrepancy for δ_l is significant. The value of δ_l is small but it is crucial in the understanding of the large quenching near the end ($d_{3/2}$-like part) of the sd shell relative to the smaller quenching near the beginning ($d_{5/2}$-like part) of the sd shell (see Table II and Fig. 1). This can be seen by using Eq. (15) with the empirical values $\delta_s = -0.32$, $\delta_l = 0.05$, and $\delta_p = 0.06$ to obtain the following:

$$\delta(5\text{-}5,\text{IS}) = -0.32 + 4 \times 0.05 + (\tfrac{4}{7}) \times 0.06 = -0.09 \ ,$$

$$\delta(3\text{-}3,\text{IS}) = -0.32 - 6 \times 0.05 + 2 \times 0.06 = -0.50 \ ,$$

and

$$\delta(5\text{-}3,\text{IS}) = -0.32 - 1 \times 0.05 + (\tfrac{1}{2}) \times 0.06 = -0.34 \ .$$

As a final comment concerning the isoscalar spin expectation value we note that the configuration-mixed wave function can be expressed in terms of the sd-shell configuration $|i,sd\rangle$ plus all remaining configurations outside the sd shell $|i,R\rangle$

$$|i\rangle = (1-a^2)^{1/2} |i,sd\rangle + a |i,R\rangle \ .$$

Since $\langle i,sd | S_Z | i,R \rangle = 0$, the spin expectation value is given by

$$\langle i \mid S_z \mid i \rangle = (1-a^2)\langle i,sd \mid S_z \mid i,sd \rangle$$
$$+a^2\langle i,R \mid S_z \mid i,R \rangle .$$

If we assume that a^2 and $\langle i,R \mid S_z \mid i,R \rangle$ are state and mass independent, then an $A = 18-38$ fit to these quantities gives $a^2 = 0.30(4)$ and

$$\langle i,R \mid S_z \mid i,R \rangle = 0.29(7)$$

with an rms of 0.053. This rms is not much larger than the rms of 0.038 obtained in the four parameter fit. From this we would conclude that the wave functions for $A = 16-40$ nuclei are only about 70% pure sd configurations. However, it is not at all clear that $\langle i,R \mid S_z \mid i,R \rangle$ should be state and mass independent, and it would be interesting to investigate the microscopic CM calculations further in this respect.

B. Isovector GT corrections

In discussing the IVM1 and GT operators it is important to note from Table V that the configuration-mixing and isobar-current corrections to the spin parts of these two operators are essentially identical, whereas the mesonic-exchange currents make larger contributions to the effective IVM1 operator than to the effective GT operator. Thus, in this section we discuss the GT operator, and leave the discussion for the more complicated IVM1 operator to Secs. V D and V E.

For the GT operator we obtain the rather small empiri-

cal upper limits of $\delta_l(GT) < 0.008$ and $\delta_p(GT) < 0.034$. These are consistent with the values of 0.008 and 0.022, respectively, which were calculated by Towner and Khanna. We note, however, that more precise information on $\delta_p(GT)$ has recently been obtained from an analysis of all GT beta decay in the sd shell[6] and from a measurement of the $A = 39$ $\frac{3}{2}^+$ to $\frac{1}{2}^+$ beta transition.[51] These new $\delta_p(GT)$ results will be published separately.[6]

For the $\delta_s(GT)$ terms, our analysis unambiguously gives quite large empirical values, as shown in Table IV. The values in Table IV incorporate our assumed $(A/28)^{0.35}$ mass dependence and are compared there with the average of the values for $A = 16$ and 40 which are calculated by Towner and Khanna. In order to simplify the discussion, the following comparisons will be made with the $A = 40$ calculations. The appropriately scaled empirical values are obtained by multiplying the values in Table IV by $(40/28)^{0.35}$ to obtain

$$\delta_s(GT,d\text{-}d) = -0.31 \pm 0.02$$

and

$$\delta_s(GT,s\text{-}s) = -0.26 \pm 0.03 \tag{25}$$

($A = 40$ empirical values). The Towner-Khanna calculations for the d and s orbits are very similar. Their $A = 40$ results for the d orbit can be decomposed into the separate CM, IC, MEC, and RE corrections. (The total given in Table V differs slightly due to roundoff error)

$$\delta_s(GT,d\text{-}d) = -0.176(CM) - 0.037(IC) + 0.018(MEC) - 0.019(RE) = -0.214 . \tag{26}$$

It is interesting to compare this to the result obtained with the prescription of Oset and Rho.[28] The Oset-Rho prescription is based on the observation that for the triton beta decay the contributions from the corrections which involve the tensor correlations (most of the contributions from the rows labeled 2, 5, and 8 in Table V) tend to can-

cel.[52-54] In the Towner-Khanna calculations this cancellation also tends to occur for $A = 3$ (see Table 7 of Ref. 1). It has been hypothesized that this cancellation persists in heavier nuclei.[54,28,55] Leaving out the contributions from the rows labeled 2, 5, and 8 in Table V, one obtains

$$\delta_s'(GT,d\text{-}d) = -0.063(CM,2\hbar\omega) - 0.039(IC, \text{ without } CP) - 0.008(MEC, \text{ without } CP) - 0.019(RE) = -0.129 . \tag{27}$$

The disagreement between the totals of Eqs. (26) and (27) means that there is not much cancellation between the omitted terms in this case.

In addition one can make the comparisons using the Oset-Rho (OR) interaction[28] for the isobaric-current calculation (IC,OR) (see Table VI)

$$\delta_s(GT,d\text{-}d) = -0.176(CM) - 0.151(IC,OR)$$
$$+0.018(MEC) - 0.019(RE)$$
$$= -0.328 , \tag{28}$$

$$\delta_s'(GT,d\text{-}d) = -0.063(CM,2\hbar\omega) - 0.151(IC,OR)$$
$$-0.008(MEC, \text{ without } CP) - 0.019(RE)$$
$$= -0.241 . \tag{29}$$

Arima et al.[47] recently investigated the reason for the large difference between the IC contributions obtained with the Towner-Khanna and Oset-Rho interactions. They conclude that the isobar calculation using the Oset-Rho (Landau-Migdal) type interaction with the value of g_Δ' reduced from 0.6 to about 0.35 is compatible with the results obtained using the Towner-Khanna one-boson exchange potential (OBEP)-type interaction.

Comparison of all of the above results with our empirical value of -0.31 ± 0.02 favors Eq. (28), in which the core-polarization and isobaric-current contributions are both important and about equal in magnitude. However, since the strength of the short-ranged part of the Oset-Rho interaction can be considered a free parameter, agreement can also be obtained within the framework of the Oset-Rho prescription [Eq. (29)] by increasing g_Δ' from 0.6 to about 0.7.

C. Isobar-current contributions to GT as deduced from a comparison of ISM1 and GT matrix elements

Within the framework of the Towner-Khanna—type calculations, a method which has been used to separate the configuration-mixing (CM) and isobar-current (IC) contributions to the quenching of the GT matrix elements involves arranging terms into the form[8,50]

$$\delta_s(GT,IC) = \delta_s(GT)_{exp} - \delta_s(GT,MEC)_{th}$$
$$- \delta_s(GT,RE)_{th} - \delta_s(GT,CM)_{th}$$
$$= \delta_s(GT)_{exp} - \delta_s(GT,MEC)_{th}$$
$$- \delta_s(GT,RE)_{th} - R\,\delta_s(IS,CM)_{th}$$
$$= \delta_s(GT)_{exp} - \delta_s(GT,MEC)_{th}$$
$$- \delta_s(GT,RE)_{th} - R\,[\delta_s(IS)_{exp}$$
$$- \delta_s(IS,MEC)_{th}] \ . \tag{30}$$

The isoscalar mesonic-exchange current (MEC) and relativistic (RE) corrections in the last lines of this expression are relatively small and can hence be estimated theoretically with fair reliability [see, however, the comments concerning $\delta_s(IS,MEC)$ in Sec. V A]. It is expected that R, the ratio

$$\delta_s(GT,CM)_{th}/\delta_s(IS,CM)_{th} \ ,$$

is less model dependent than is either of these quantities individually. For example, R would not depend upon the overall strength of the two-body interactions used for the CM calculations. Thus, Eq. (30) relates the quantity of interest on the left-hand side, the IC correction to a combination of experimental and relatively well understood theoretical quantities on the right-hand side.

The numerical results for the d and s orbits are [the numbers in parentheses ( ) indicate the experimental errors]

$$\delta_s(GT,IC,d\text{-}d) = [-0.31(2)] - [+0.018] - [-0.019] - 0.43\{[-0.36(5)] - [+0.050]\}$$
$$= -0.13 \pm 0.03 \ ,$$
$$\delta_s(GT,IC,s\text{-}s) = [-0.26(3)] - [+0.018] - [-0.019] - 0.44\{[-0.15(10)] - [+0.045]\}$$
$$= -0.17 \pm 0.05 \ , \tag{31}$$

where the order of the numbers is the same as the order of the terms in Eq. (30). The theoretical values for the $\delta_s(IS,MEC)$ and $\delta_s(GT,RE)$ are taken from the $A=40$ calculations in Table V, and the experimental numbers are our empirical results from Table IV, scaled to $A=40$ by multiplying them by $(40/28)^{0.35} = 1.13$. The results of the Towner-Khanna calculation,

$$\delta_s(GT,IC,d\text{-}d) = -0.037$$

and

$$\delta_s(GT,IC,s\text{-}s) = -0.041$$

(see Table V), are at least a factor of 2 smaller than the values given by Eq. (31). Put in another way, the agreement between experiment and theory for the isoscalar moments indicates that the CM calculations are basically correct. It follows from this that since the empirically deduced GT quenching is larger than that obtained in the Towner-Khanna calculations, the calculated values of the IC corrections are probably too small.

D. Comparisons of the isovector M1 and GT corrections

It is interesting to compare the differences in the empirical corrections δ_s for the GT and IVM1 cases. In the calculations of Towner and Khanna these differences are seen to arise nearly exclusively from the MEC corrections, for the reasons discussed above. The differences in the empirical corrections (see Table IV) are

$$\delta_s(GT,d\text{-}d) - \delta_s(IVM1,d\text{-}d) = 0.16 \pm 0.04 \ ,$$

$$\delta_s(GT,s\text{-}s) - \delta_s(IVM1,s\text{-}s) = 0.23 \pm 0.05 \ .$$

The constancy of this difference as a function of mass shows up clearly in the ratios plotted at the bottom of Fig. 1. This effect has also been indicated in our previous sd-shell comparisons with the Chung-Wildenthal interaction,[9] in the p-shell comparisons of Yoro,[56] and in a recent study of particle-hole states near ^{16}O.[57]

The Towner-Khanna calculations give values which, while significantly larger than previous calculated values, are only about half the empirical values:

$$\delta_s(GT,d\text{-}d) - \delta_s(IVM1,d\text{-}d) = 0.091 \ ,$$

$$\delta_s(GT,s\text{-}s) - \delta_s(IVM1,s\text{-}s) = 0.088 \ .$$

From Table V it can be seen that the first order MEC contribution contributes only about half of the theoretical values and that the higher-order MEC corrections induced by the tensor interaction are again important. Delorme[24] recently obtained a Fermi-gas model result of 0.14 for this difference, which agrees fairly well with the Towner-Khanna calculation for deeply-bound orbitals.

E. Orbital isovector M1 correction

From our fits we have obtained for the correction to the orbital IVM1 operator

$$\delta_l(\text{IVM1}) = 0.013 \pm 0.008 \ . \tag{32}$$

At present the error is large but we expect this error in the sd shell to be reduced when we include in our analysis data on $M1$ transitions.[6] Expressed as a percentage correction to $g_l(\text{IVM1})$ our result is $100 \times 9.41 \times (0.013 \pm 0.008) = 12 \pm 8$.

This result is very significant in comparison with the Towner-Khanna calculations. Their $(A=40)$ configuration mixing result alone gives a value (see Table V) of

$$\delta_l(\text{CM,IVM1}) = -0.049 \ , \tag{33}$$

which is completely inconsistent with our empirical result of 0.013 ± 0.008. However, their mesonic-exchange-current correction is also large and has the opposite sign,

$$\delta_l(\text{MEC,IVM1}) = 0.059 \ . \tag{34}$$

It is only by this delicate cancellation between these two contributions that agreement with the empirical value is obtained.

VI. CONCLUSIONS AND FUTURE DEVELOPMENTS

We have established in this study that GT and $M1$ data from nuclear states in the $A=18-38$ region are, at the least, as consistent with the predictions of many-particle, configuration-mixed wave functions as the same types of data for the ground states of $A=17$ and 39 are with the equivalent predictions of the single-particle model. The empirical values of the higher-order corrections to the free-nucleon values of the GT and $M1$ single-particle matrix elements which we extract from the $A=18-38$ data are reasonably consistent with the analogous corrections which can be extracted from the $A=17$ and 39 data. Our analysis of multiparticle data yields a more complete set of corrections than can be obtained from the single-particle systems alone, however, and also, importantly, yields a quantitative measure of the uncertainties in the values of these corrections. Inspection of the overall $A=17-39$ results (see Tables II and III and Fig. 1) suggests that the internal consistency of the $A=18-38$ data is greater than that of the composite $A=17+39+18-38$ data. We hence conclude that the combination of the results of our analysis of multiparticle systems to the results obtained for the single-particle systems significantly expands and consolidates our empirical knowledge of higher-order corrections to the GT and $M1$ operators.

The empirical values we extract for the higher-order corrections to the GT and $M1$ operators are generally consistent overall with the theoretical values obtained by Towner and Khanna in a comprehensive calculation of such effects. Thus, the experimental values of GT and $M1$ observables appear to be theoretically comprehensible even in subtle details. This combination of results should significantly advance our confidence in the basic elements of nuclear-structure theory. This advance is principally a consequence of carrying out the necessary shell-model and perturbation-theory calculations more systematically.

Some further improvements in the empirical determination of the effective $M1$ and GT operators are straightforward to accomplish and will be soon forthcoming.[6] These improvements will involve the inclusion in our analysis of essentially all experimental data on sd-shell GT beta-decay transitions and $M1$ gamma-decay transitions. Many of these transitions are more sensitive than are the moments to the off-diagonal single-particle matrix elements, and thus these analyses will be more sensitive to the δ_p terms in Eq. (11). Also, as noted, the present restricted and cross-correlated data sets can be significantly expanded by additional experimental measurements of magnetic moments; particularly important are those of ^{28}P, ^{30}P, ^{33}Cl, ^{37}Ar, and ^{37}K.

Further improvement in the shell-model theory will require a further refinement of the sd-shell Hamiltonian. Such improvements should remove some of the ambiguity existing at present, for example, in the interpretation of the $A=29$ and 31 moments. It will be equally, if not more important, however, to consider the explicit two-body operators which arise theoretically in the calculation of the higher-order corrections. An indication of the importance of a two-body operator effect can be seen in the lower panel of Fig. 1. The ratios of the experimental to theoretical GT matrix elements show a persistent odd-even staggering, both with the free-nucleon operators and with the empirical operators. Such a staggering is reminiscent of two-body operator effects as exhibited, for example, in nuclear binding energies. The technical aspects of calculating the $\Delta J=1$ two-body transition densities have recently been solved.[58] However, there remains the problem of determining the form of the two-body operator from the higher-order calculations. The operator can be readily obtained for the zeroth-order isobar and mesonic-exchange currents (see, for example, Refs. 20 and 37). However, the operator for the higher-order configuration mixing is not known.

In the comparisons with the calculations of Towner and Khanna[1] we have noted the overall good agreement with our empirical operators. The calculations still need some improvement, and we have suggested that part of this could involve an increase in the contribution of the isobaric currents in their calculation. In many cases it has been seen that there are rather delicate cancellations between the configuration mixing, isobar-current, and mesonic-exchange-current contributions. These cancellations have been noted in previous work of Arima et al.[3] It would obviously be a major step in simplifying the calculations if these cancellations could be understood more fundamentally along the lines outlined by Rho.[55] This would facilitate their extension to more diverse phenomena such as electron scattering form factors.

18CORRECTIONS TO THE FREE-NUCLEON VALUES OF THE . . .2413

[1] I. S. Towner and F. C. Khanna, Nucl. Phys. A399, 334 (1983).

[2] K. Shimizu, M. Ichimura, and A. Arima, Nucl. Phys. A226, 282 (1974).

[3] A. Arima, H. Hyuga, and K. Shimizu, in *Mesons in Nuclei,* edited by M. Rho and D. H. Wilkinson (North-Holland, Amsterdam, 1979).

[4] H. Hyuga, A. Arima, and K. Shimizu, Nucl. Phys. A336, 363 (1980).

[5] B. H. Wildenthal and W. Chung, in *Mesons in Nuclei,* edited by M. Rho and D. H. Wilkinson (North-Holland, Amsterdam, 1979), p. 723.

[6] B. A. Brown and B. H. Wildenthal (unpublished).

[7] D. H. Wilkinson, Nucl. Phys. A209, 470 (1973).

[8] D. H. Wilkinson, Nucl. Phys. A225, 365 (1974).

[9] B. A. Brown, W. Chung, and B. H. Wildenthal, Phys. Rev. Lett. 40, 1631 (1978).

[10] B. H. Wildenthal, Bull. Am. Phys. Soc. 27, 725 (1982).

[11] D. H. Wilkinson and B. E. F. Macefield, Nucl. Phys. A232, 58 (1974).

[12] B. H. Wildenthal, M. S. Curtin, and B. A. Brown, Phys. Rev. C 28, 1343 (1983).

[13] R. G. Sachs, Phys. Rev. 69, 611 (1946).

[14] K. Sugimoto, Phys. Rev. 182, 1051 (1969).

[15] P. C. Zalm, J. F. A. van Heinen, and P. W. M. Glaudemans, Z. Phys. A 287, 255 (1978).

[16] B. A. Brown, J. Phys. G 8, 679 (1982).

[17] H. Miyazawa, Prog. Theor. Phys. 6, 801 (1951).

[18] M. Chemtob, Nucl. Phys. A123, 449 (1969).

[19] S. Wahlborn and J. Blomqvist, Nucl. Phys. A133, 50 (1969).

[20] M. Chemtob and M. Rho, Nucl. Phys. A163, 1 (1971).

[21] A. Barroso and R. J. Blin-Stoyle, Nucl. Phys. A251, 446 (1975).

[22] G. Konopka, M. Gari, and J. G. Zabolitzsky, Nucl. Phys. A290, 360 (1977).

[23] C. Bargholtz, Phys. Lett. 81B, 286 (1979).

[24] J. Delorme, Nucl. Phys. A374, 541 (1982).

[25] T. Erikson, Phys. Lett. 43B, 453 (1973).

[26] M. Rho, Nucl. Phys. A231, 493 (1974).

[27] K. Ohta and M. Watamatsu, Nucl. Phys. A234, 445 (1974).

[28] E. Oset and M. Rho, Phys. Rev. Lett. 42, 47 (1979).

[29] W. Knupfer, M. Dillig, and A. Richter, Phys. Lett. 95B, 349 (1980).

[30] H. Toki and W. Weise, Phys. Lett. 97B, 12 (1981).

[31] A. Bohr and B. R. Mottelson, Phys. Lett. 100B, 10 (1981).

[32] A. Harting, W. Weise, H. Toki, and A. Richter, Phys. Lett. 104B, 261 (1981).

[33] T. Suzuki, S. Krewald, and J. Speth, Phys. Lett. 107B, 9 (1981).

[34] G. E. Brown and M. Rho, Nucl. Phys. A372, 397 (1981).

[35] H. Sagawa and N. van Giai, Phys. Lett. 113B, 119 (1982).

[36] M. Kohno and D. W. L. Sprung, Phys. Rev. C 26, 297 (1982).

[37] R. D. Lawson, Phys. Lett. B (to be published).

[38] M. Ichimura and K. Yazaki, Nucl. Phys. 63, 401 (1965).

[39] H. A. Mavromatis and L. Zamick, Phys. Lett. 20, 191 (1966).

[40] H. A. Mavromatis and L. Zamick, Nucl. Phys. A104, 19 (1967).

[41] G. F. Bertsch, Phys. Lett. 28B, 302 (1968).

[42] T. Erikson, Nucl. Phys. A205, 593, (1973).

[43] J. S. Bell and R. J. Blin-Stoyle, Nucl. Phys. 6, 87 (1957).

[44] H. Ohtsubo, M. Sano, and M. Morita, Prog. Theor. Phys. 49, 877 (1973).

[45] N. C. Mukhopadhyay and L. D. Miller, Phys. Lett. 47B, 415 (1973).

[46] I. S. Towner and F. C. Khanna (private communication).

[47] A. Arima, T. Cheon, K. Shimizu, H. Hyuga, and T. Suzuki, Phys. Lett. 122B, 126 (1983).

[48] J. H. D. Jensen and M. Goeppert-Mayer, Phys. Rev. 85, 1040 (1952).

[49] A. Bohr and B. R. Mottelson, *Nuclear Structure* (Benjamin, New York, 1969), Vol. I.

[50] S. Raman, C. A. Houser, T. A. Walkiewicz, and I. S. Towner, At. Data Nucl. Data Tables 21, 567 (1978).

[51] E. G. Adelberger, J. L. Osborne, H. E. Swanson, and B. A. Brown, submitted to Phys. Rev. C.

[52] A. M. Green and T. H. Schucan, Nucl. Phys. A188, 289 (1972).

[53] M. Ichimura, H. Hyuga, and G. E. Brown, Nucl. Phys. A196, 17 (1972).

[54] M. Rho, in *Progress in Particle and Nuclear Physics,* edited by D. H. Wilkinson (Pergamon, New York, 1976).

[55] M. Rho, *Common Problems in Low- and Medium-Energy Nuclear Physics,* edited by B. Castel, B. Goulard, and F. C. Khanna (Plenum, New York, 1979).

[56] K. Yoro, Phys. Lett. 70B, 147 (1977).

[57] K. A. Snover, E. G. Adelberger, P. K. Ikossi, and B. A. Brown, Phys. Rev. C 27, 1837 (1983).

[58] B. A. Brown (unpublished).

[59] A. R. Admonds, *Angular Momentum in Quantum Mechanics* (Princeton University Press, Princeton, N.J., 1960).

[60] P. M. Endt and C. van der Leun, Nucl. Phys. A310, 1 (1978).

[61] J. W. Hugg, D. L. Clark, J. R. Hall, S. J. Freedman, B. B. Triplet, and S. S. Hanna, Bull. Am. Phys. Soc. 23, 929 (1978).

[62] R. A. Smith and V. R. Pandharipande, Nucl. Phys. A256, 327 (1976).